# Synthesis and Characterization of Polyimide/ Multi-Walled Carbon Nanotube Nanocomposites

**Te-Cheng Mo,[1] Hong-Wen Wang,[2] San-Yan Chen,[1] Yun-Chieh Yeh[2]**
[1]*Department of Materials Science and Engineering, National Chiao-Tung University, Hsinchu, 30049, Taiwan, Republic of China*

[2]*Department of Chemistry, Chung-Yuan Christian University, Chungli 32023, Taiwan, Republic of China*

**Polyimide/multi-walled carbon nanotube (PI-MWNT) nanocomposites were fabricated by an in situ polymerization process. Chemical compatibility between the PI matrix and MWNTs is achieved by pretreatment of the carbon nanotubes in a mixture of sulfuric acid and nitric acid. The dispersion of MWNTs in the PI matrix was found to be enhanced significantly after acid modification. The glass transition ($T_g$) and decomposition ($T_d$) temperature of PI-MWNT nanocomposites were improved as the MWNT content increased from 0.5 to 15 wt%. The storage modulus of the PI/MWNT nanocomposites is nine times higher than that of pristine PI at room temperature. The tensile strength of PI doubles when 7 wt% MWNTs is added. The dielectric constant of the PI-MWNT nanocomposites increased from 3.5 to 80 (1 kHz) as the MWNT content increased to 15 wt%. The present study demonstrates that enhanced mechanical properties can be obtained through a simple in-situ polymerization process. POLYM. COMPOS., 29:451–457, 2008. © 2008 Society of Plastics Engineers**

## INTRODUCTION

Carbon nanotubes (CNTs) have attracted considerable attention because of their unique structural, electrical, and mechanical properties [1]. Multi-walled carbon nanotubes (MWNTs) have been used in composite materials to improve electrical properties while reinforcing the mechanical performance of the composites [2–9]. Compared with traditional reinforcing agents such as glass fibers, CNTs are much more efficient in improving the composite properties because of their extremely high aspect ratio. However, achieving a high degree of dispersion of MWNTs in a polymer matrix is challenging due to agglomeration and aggregation into bundles. Phase separation leads to heterogeneous dispersion in the polymer matrix and poor properties of the resulting composites. Special care must be taken in order to fabricate composites with CNTs homogeneously distributed throughout the polymer matrix. Uniform dispersion within the polymer matrix and improved nanotube-matrix wetting and adhesion has been critical issue in the processing of the nanocomposites. By gelation/crystallization from solution, Matsuo and coworkers [10–12] were able to produce composites of polyacrylonitrile/MWNTs, polyethylene/MWNTs, and EMMA copolymer/MWNTs with exceptionally high mechanical properties. However, sophisticated processing is required for this method. To achieve homogeneous dispersion of MWNTs in polymer matrix by facile mixing, chemically treated MWNTs have been employed. Chemically functionalized CNTs treated by strong mixed acid were found to be soluble in amide solvents [13]. MWNTs modified by strong acid contain carboxyl and hydroxyl groups on the surface. These groups enhance the interactions between the CNTs and the polymer matrix, enabling uniform dispersion of MWNTs without boundary effects in the polymer matrix [13]. Zhu et al. [14] disclosed the thermal, mechanical, and electrical properties of PI-MWNT nanocomposites with increasing MWNT content. They demonstrated a slightly decreased thermal stability for the PI-MWNT nanocomposites due to acid treatment. For PI-MWNTs with a MWNT content above 5 wt%, the tensile strength was increased by 40% and then declined [14]. Jiang et al. [15] even concluded that there is no significant improvement in mechanical properties for PI-MWNTs nanocomposites by in situ polymerization. Since the addition of MWNTs was expected to reinforce mechanical properties in most polymer-MWNT systems, it is worthwhile to carry out a more detailed study on this interesting system. In addition, the dielectric properties and TEM data have not been well studied. This report characterizes PI-MWNT nanocomposites (0.25–15 wt% MWNTs) and presents their mechanical, thermal, moisture absorption, conductivity, and dielectric properties.

*Correspondence to*: Hong-Wen Wang; e-mail: hongwen@cycu.edu.tw
Contract grant sponsor: National Science Council, Taiwan, Republic of China; contract grant number: NSC 94-2113-M-033-004.
DOI 10.1002/pc.20468
Published online in Wiley InterScience (www.interscience.wiley.com).

## EXPERIMENTAL

MWNTs were purchased from Carbon Solutions. The MWNTs have outer diameters of 40–60 nm and lengths of 0.5–500 $\mu$m. The modified MWNTs were prepared by ultrasonicating the mixture of MWNTs in sulfuric acid and nitric acid (volumetric ratio 3:1) at 45°C for 24 h, centrifuging washing with water and drying in a vacuum oven at 80°C for 24 h. Polyimide precursors such as DBPA and 4,4-oxydianiline (ODA) were purchased from Aldrich. *N*,*N*-dimethylacetamide (DMAc Tedia 99%) was used as a solvent. For a typical synthesis process, 3 g DMAc and the appropriate amount (from 0.25 to 15 wt%) of acid-oxidized MWNTs were placed in a beaker and stirred under ultrasonication for 24 h at room temperature to reach a homogenous suspension (beaker A). About 1 nmole ODA and 1.5 g DMAc were placed in another beaker and stirred for 15 min (beaker B). Next, the solutions of beakers A and B were combined and stirred for 24 h. Finally, 1 nmole dianhydride ($C_{31}H_{20}O_8$) was dissolved in 1.5 g DMAc and stirred for 15 min (beaker C). Beaker C was added to the beaker A + B mixture and stirred for 24 h. The nanocomposite films were prepared by coating 3 ml of the final mixture solution on a piece of 50 mm × 50 mm glass slide. The resultant films were dried in an oven and subsequently imidized at high temperature in air. The imidization process was completed in a heating program shown as follow: ramping from room temperature to 80°C in 30 min, keeping at 80°C for 2 h, then ramping from 80 to 200°C in 5 h, and then from 200 to 300°C in 2 h, keeping at 300°C for 45 min, and finally cooling to room temperature. The imidization process was finalized by many experiments in our laboratory.

A wide-angle X-ray diffraction (WAXRD) study was performed using a Rigaku D/MAX-3C X-ray diffractometer with a copper target and a Ni filter at a scanning rate of 2°/min. The samples for the transmission electron microscopy (TEM) study were taken from a microtomed section of polyimide-MWNT nanocomposites (~75 ± 15 nm in thickness) and mounted in a resin. A JEOL-2010 TEM with an acceleration voltage of 200 kV was employed for the observation. Thermal gravimetric analysis (TGA) scans were performed in air on a Mettler-Toledo TGA/SDTA851 thermal analysis system. The scan rate was 20°C/min and the temperature range was from 30 to 900°C. Differential scanning calorimetry (DSC) was performed on a DuPont TA Q10 differential scanning calorimeter at a heating or cooling rate of 10°C/min in a nitrogen atmosphere from 25 to 350°C. The glass transition temperature ($T_g$) of polyimide and the synthesized nanocomposites were recorded based on the second scan. Dynamic mechanical analysis (DMA) of the polyimides and nanocomposite films was performed from 30 to 350°C using a DuPont TAQ800 analyzer at a heating rate of 3°C/min and a frequency of 1 Hz. Dielectric parameters such as capacitance and the dissipation factor (tan $\delta$) were measured by an Agilent 4284A automatic component analyzer at various frequencies (1 kHz to 1 MHz) at temperatures of 35–150°C. A vacuum evaporated gold electrode was deposited on both sides of the nanocomposite films (1.6 cm in diameter). Specimens with a thickness of about 100 ± 5 $\mu$m were prepared. Film thickness was measured using a micrometer (precision up to 0.001 mm). Five data points from different areas of the specimen were taken and averaged for the calculation of the dielectric constants. Films with thickness deviation less than 5% were used for dielectric characterization. The dielectric constants ($\varepsilon_r$) were calculated by the equation: $C = \varepsilon_r \varepsilon_0 A/d$. "$\varepsilon_0$" is vacuum permittivity and equals $8.85 \times 10^{-12}$ F/m. "$A$" is the electrode area and "$d$" is the thickness of the specimen. To exclude the effect of moisture, specimens for dielectric characterization were dried in an oven at 100°C for 2 h before the measurements. To evaluate the moisture absorption of nanocomposites, the film specimens were vacuum dried at 80°C for 24 h and then weighed ($W_a$). The film specimens were subsequently immersed in deionized water for 24 h at room temperature for water absorption characterization. The excess water on the surface of film specimens was wiped using a delicate-task paper wiper (Kimberly-Clark) before weighing again ($W_b$). Moisture absorption was calculated using the formula $(W_b - W_a)/W_a \times 100\%$. The tensile strength was measured on an MTS-8800 tensile tester based on ASTM D638 specification and the tensile rate was 1 mm/min at room temperature.

## RESULTS AND DISCUSSION

### *XRD*

The structure of polyimide/MWNT nanocomposites was examined by XRD and the resultant curves are shown in Fig. 1. MWNTs and pristine PI were also investigated and compared. For the MWNTs, two peaks appear at $2\theta = 26°$ and 43° which correspond to the interlayer spacing

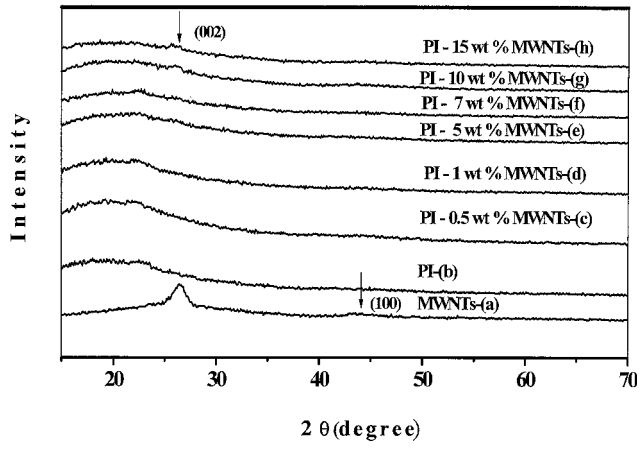


FIG. 1. XRD patterns for (a) MWNTs, (b) pristine PI, and (c)–(h) PI-MWNT nanocomposites containing 0.5, 1, 5, 7, 10, and 15 wt% MWNTs, respectively.


DOI 10.1002/pc

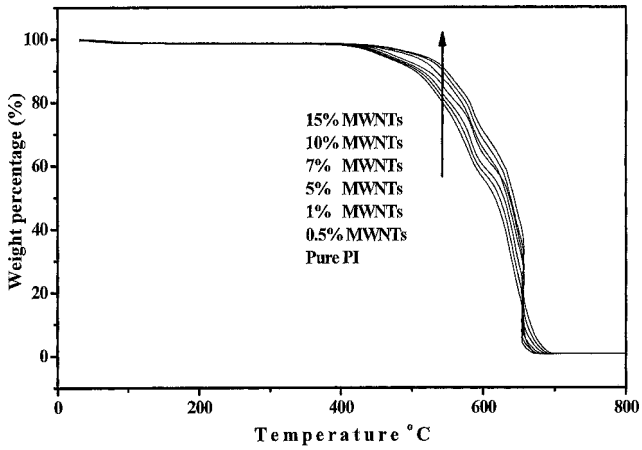


FIG. 2. TGA curves for pure PI and the PI-MWNT nanocomposites.

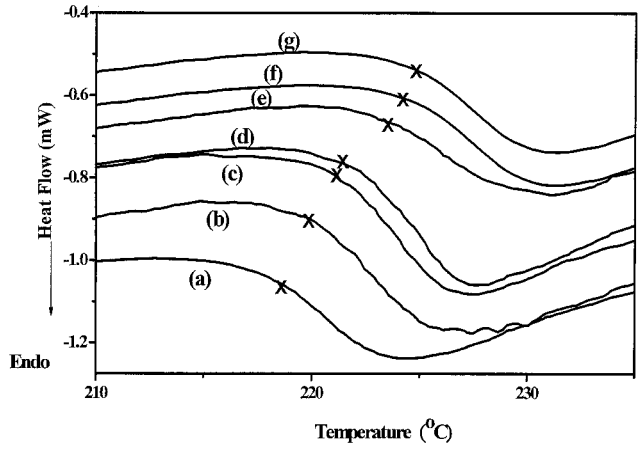


FIG. 3. DSC of the PI-MWNT nanocomposites: (a) Pure PI, (b) PI-0.5 wt% MWNTs, (c) PI-1 wt% MWNTs, (d) PI-5 wt% MWNTs, (e) PI-7 wt% MWNTs, (f) PI-10 wt% MWNTs, (g) PI-15 wt% MWNTs.

$d_{(002)}$ and $d_{(100)}$ reflection of the nanotubes, respectively [9]. For the pristine PI, an obvious broad peak centered at $2\theta = 17.5^\circ$ indicates the PI (BPDA/ODA) polymer is amorphous. For the MWNT content higher than 10 wt%, the PI-MWNT nanocomposites exhibit peaks of PI and MWNTs, as show in Fig. 1g and h. The intensity of the peaks assigned to the MWNTs in the nanocomposites increases with an increasing proportion of MWNTs.

*Thermal Properties and Moisture Absorption*

Figure 2 shows the TGA curves obtained in air for the studied polyimide/MWNT nanocomposites. In Fig. 2, the onset of $T_d$ (decomposition temperature) of the PI-MWNTs is higher than that of pristine PI and it shifts toward higher temperatures as the amount of MWNTs is increased. The $T_d$ of pristine PI and the PI-MWNT nanocomposites with increasing amount of MWNTs such as 0.5, 1, 5, 7, 10, 15 wt% are ~490.5, 493.2, 495.4, 498.7, 501.3, 503.4, and 505.5°C, respectively, as listed in Table 1. The $T_d$ of the nanocomposite with 15 wt% MWNTs exhibits a $T_d$ 15°C higher than that of pristine PI. It is clear that the PI-MWNT materials improve thermal stability due to the incorporation of MWNTs. DSC thermograms for pristine PI and the series of PI-MWNT materials are shown in Fig. 3. Pristine PI exhibits an endothermic peak at ~218.1°C, corresponding to the glass transition temperature ($T_g$) of PI. The $T_g$ for the PI-MWNT nanocomposites shown in Fig. 3 according to increasing MWNT content are ~219.7, 221.5, 222.4, 223.9, 224.3, and 225.2°C, as shown in curves (b) to (g), respectively. The $T_g$ of PI-MWNT materials are only slightly different from that of pristine PI, and the change in $T_g$ due to the addition of MWNTs seems small. The details of the thermal properties are tabulated in the Table 1. The result suggests that the secondary network structure is formed by the MWNTs in addition to the primary crosslink structure of the polymers, and the MWNTs are immobilizing the polymer chains at elevated temperatures [16]. Low moisture absorption is required for materials applied in microelectronic devices. Polar groups in polymer tend to absorb moisture. Therefore, the moisture absorption of PI-MWNT nanocomposites must be examined. As shown in Table 1, the moisture absorption moderately increases from 1.25 to 1.42% as the content of MWNTs increases from 0 to 15%. The addition of MWNTs slightly affects the moisture absorption of the PI polymer due to the hydrophilic characteristics of the modified MWNTs.

*Mechanical Properties*

It has been generally accepted that incorporating nanoparticles or nanomaterials into polymer bulk improves the

TABLE 1. Thermal degradation temperature ($T_d$) and glass transition temperature ($T_g$) of PI-MWNT nanocomposites.

| Sample | $T_d$ (°C) measured by TGA | $T_g$ (°C) measured by DSC | $T_g$ (°C) measured by DMA | Moisture absorption (%) |
|---|---|---|---|---|
| Pure PI | 490.5 | 218.1 | 220.8 | 1.25 |
| PI-0.5wt% MWNTs | 493.2 | 219.7 | 221.8 | 1.29 |
| PI-1wt% MWNTs | 495.4 | 221.5 | 223.4 | 1.30 |
| PI-5wt% MWNTs | 498.7 | 222.4 | 224.5 | 1.39 |
| PI-7wt% MWNTs | 501.3 | 223.9 | 227.6 | 1.40 |
| PI-10wt% MWNTs | 503.4 | 224.3 | 228.2 | 1.41 |
| PI-15wt% MWNTs | 505.4 | 225.2 | 229.9 | 1.42 |

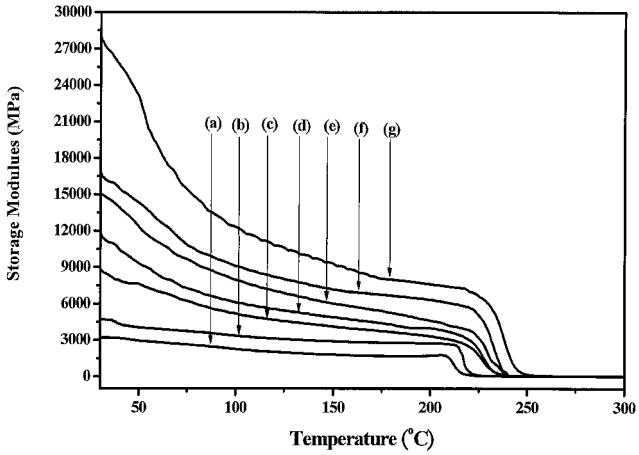


FIG. 4. Storage modulues of PI-MWNT nanocomposites at various temperatures. (a) pure PI, (b) PI-0.5 wt% MWNTs, (c) PI-1 wt% MWNTs, (c) PI-5 wt% MWNTs, (e) PI-7 wt% MWNTs, (f) PI-10 wt% MWNTs, and (g) PI-15 wt% MWNTs.

mechanical properties of nanocomposites over the polymers themselves [17–19]. However, the nanoparticles or nanomaterials benefit the mechanical properties only when they are well distributed in the polymer bulk. In this study, MWNTs were found to greatly enhance the mechanical properties of polyimide, higher than what was expected from the literature [14, 15]. Figure 4 shows the storage modulus for PI-MWNT nanocomposites with increasing MWNT contents. It is clear that the storage modulus of the nanocomposites increases with the amount of MWNTs. The maximum value of 28,457 MPa for the specimen with 15% MWNT loading is about nine times higher than that of the pristine polyimide. The improvement in storage modulus is thought to be due to the strong interactions between the polyimide matrix and MWNTs. Figure 5 shows the tensile strength and elongation at break for the PI-MWNT nanocomposite specimens. It is clear that the tensile strength of PI-MWNT

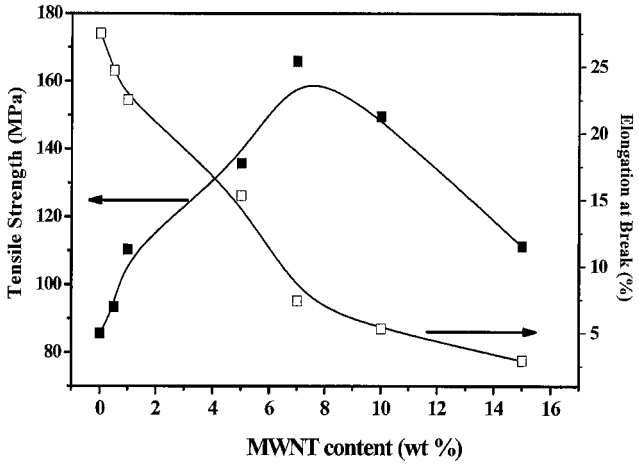


FIG. 5. Tensile strength and elongation at break of the PI-MWNT nanocomposites according to MWNT content.

nanocomposites increased as the MWNT content increased up to 7 wt%. The maximum tensile strength of 165.5 MPa for the specimen with 7 wt% MWNTs is almost double the pristine PI (85.5MPa). In Zhu et al.'s report [14], they did not have the 7 wt% data and only a 40% enhancement of tensile strength was obtained at 5 wt% MWNTs. The present study illustrates that the dispersion of MWNTs is likely to be the major factor in enhancing tensile strength.

### *Microstructure*

Observations of the morphologies of the acid-modified MWNTs are shown in Figure 6A and B. The dispersion of unmodified MWNTs was poor and the structure was aggregated. The structure of acid-modified MWNTs was loose and these dispersed better in the polymer than unmodified MWNTs. A typical TEM microstructure for the PI-5 wt% MWNT nanocomposites is presented in Fig. 6C, where well-dispersed MWNTs are observed. The greatly improved dispersion of MWNTs is due to the strong interfacial interactions and chemical compatibility between the polyimide matrix and the modified MWNTs which are caused by the strong interactions between the carboxyl and hydroxyl group of the MWNTs and the PAA molecules [20]. The enhanced mechanical properties we obtained are due to the characteristics of the MWNTs used. The extremely different length of the MWNTs (0.5–500 $\mu$m) used in the present study is likely to be the major cause for the enhanced mechanical properties. Crack propagation could be hindered by long MWNTs, which could lead to a higher tensile strength. For the PI-10 wt% MWNT nanocomposites, the distribution of MWNTs is still uniform, however, contact is inevitable, as shown in Fig. 6B. The film specimens of PI-10 wt% MWNT nanocomposites were rigid. Decreased elongations at break were observed, as shown in Fig. 5. This is likely a consequence from tangling of the MWNTs which are clear in Fig. 6D.

### *Conductivity and Dielectric Properties*

Figure 7 shows the alternative current (AC) conductivity (real part) of the PI-MWNT nanocomposites at 150°C. As expected, conductivity increases as the content of MWNTs increases and is higher at high frequencies [21]. The frequency dependence of the AC conductivity follows the "universal dynamic response" (UDR) (a power law behavior) [22, 23], which was noted by Jonscher [22]. However, the slope becomes flat at 15 wt% MWNTs, which indicates the characteristics of a conductor. The independence of frequency was also observed in other polymer-CNT systems above the percolation threshold [21, 23]. This is due to the transformation from an insulator to a conductor. The conductivity, $\sigma'(\omega \rightarrow 0) \cong \sigma_{dc}$, is a measure of the long range movements of the charge carriers corresponding to the electrical response of the percolating


DOI 10.1002/pc

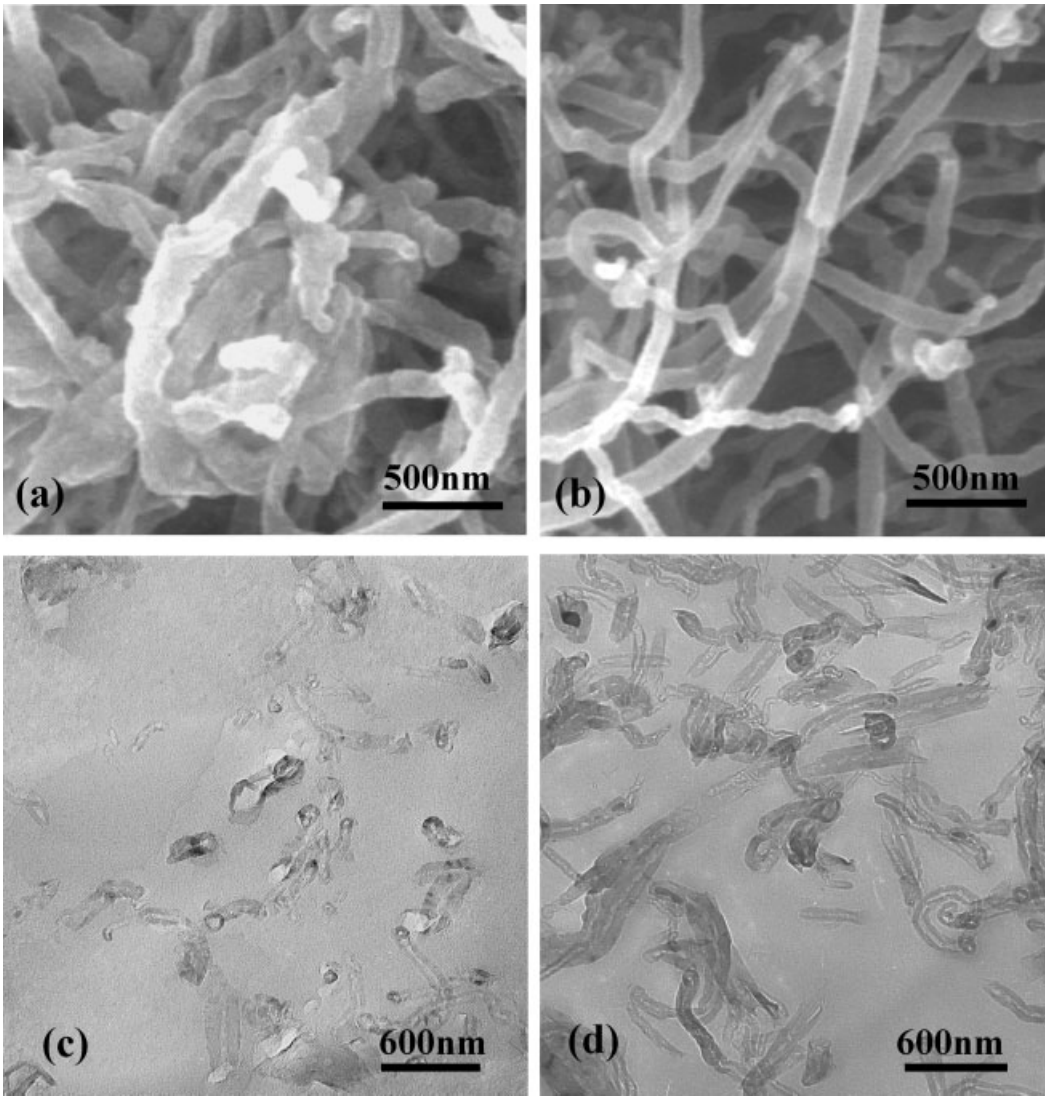


FIG. 6. SEM micrographs for (a) Un-modified MWNTs, (b) Modified MWNTs and TEM micrograph for (c) PI-5 wt% MWNT nanocomposites, and (d) PI-10 wt% MWNT nanocomposites.

network. Figure 8A and B show the dielectric constants and dielectric losses, respectively, of the PI-MWNT nanocomposites at 35–150°C and a frequency of 1 MHz. The

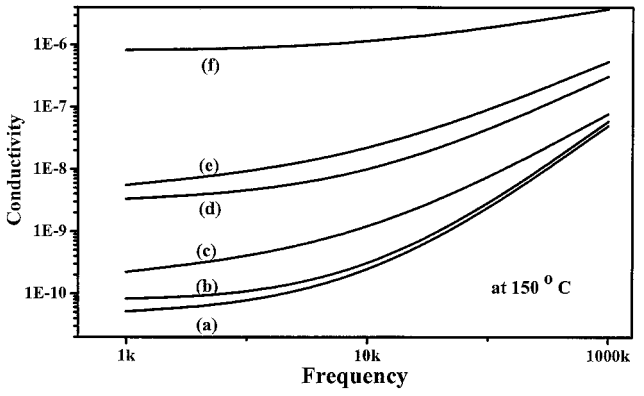


FIG. 7. ac conductivity of PI-MWNT nanocomposites at 150°C. (a) 1 wt%, (b) 3 wt%, (c) 5 wt%, (d) 7 wt%, (e) 10 wt%, (f) 15 wt%.

dielectric constants and losses exhibit stable and flat characteristics over a range of temperature. However, the dielectric constant and loss increases steadily as the loading of MWNTs in the nanocomposites increases. Figure 9A and B show the dielectric constants and dielectric losses versus various MWNT contents measured at three major frequencies, i.e. 1 kHz, 10 kHz, and 1 MHz. As shown in Fig. 9A, two increasing slopes of dielectric constants were identified. When the content of MWNTs is lower than 10 wt%, the increase of the dielectric constants is small and not significant. For the PI-MWNT nanocomposites with 10–15 wt% MWNTs, the dielectric constants and losses increase sharply. This slop is steeper at low frequencies such as 1 kHz. The slop of the increasing dielectric constant versus MWNT content becomes less steep as the frequency increased. The electrical properties of the composite obviously vary from those of an insulating material to those of a conducting system depending on the concentration of MWNTs. The high

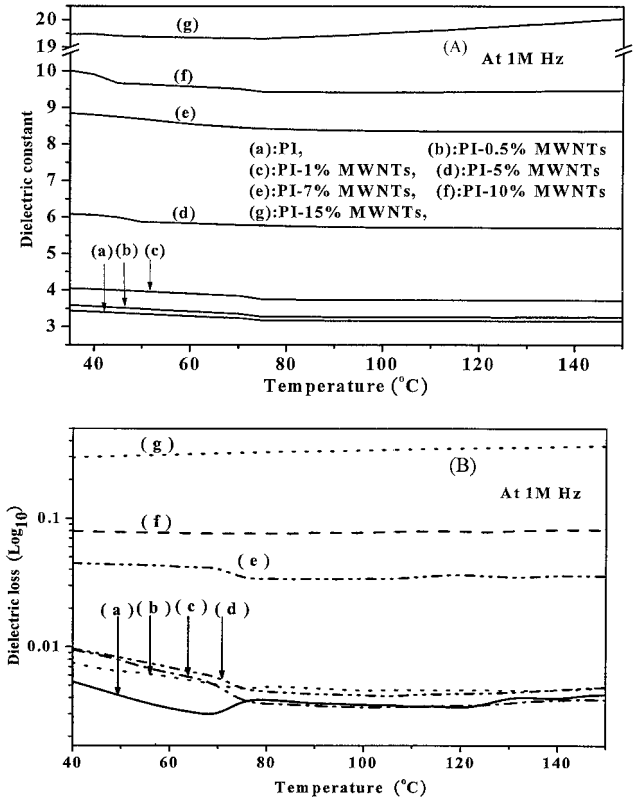


FIG. 8. (A) Dielectric constants and (B) Dielectric loss of the PI-MWNT nanocomposites at 1 MHz under various temperatures. (a) pristine PI, (b) PI-0.5 wt% MWNTs, (c) PI-1 wt% MWNTs, (d) PI-5 wt% MWNTs, (e) PI-7 wt% MWNTs, (f) PI-10 wt% MWNTs, and (g) PI-15 wt% MWNTs.

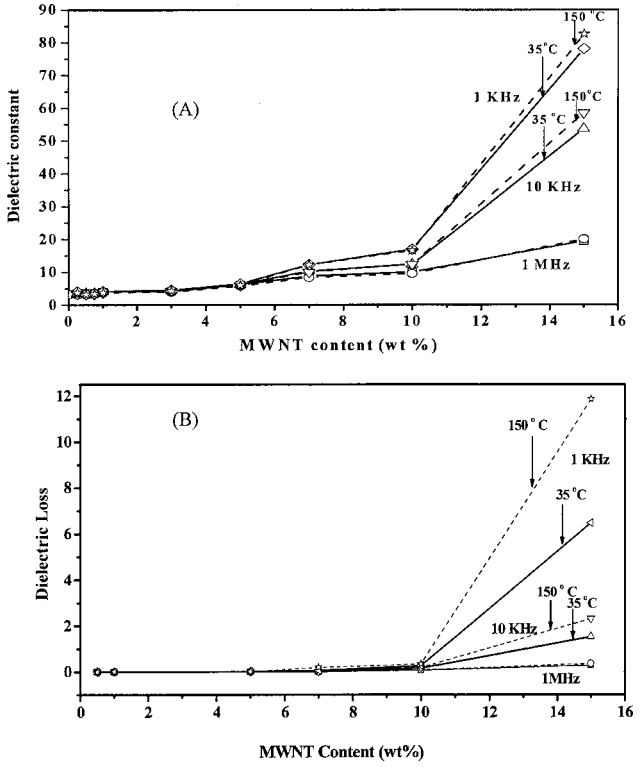


FIG. 9. (A) Dielectric constants and (B) dielectric loss of PI-MWNT nanocomposites versus the content of MWNTs (measured at 1 KHz, 10 KHz, and 1 MHz at 35, and 150°C).

dielectric constant and loss at a low frequency (1 kHz) is thought to originate from the space charge polarization mechanism [24]. The rapid increase of the dielectric constant and loss at a high MWNT content (>10 wt%) can be explained by the formation of a percolative path of the conducting network through the sample for a concentration corresponding to the percolation threshold [25–28]. In these PI/MWNTs nanocomposites, the percolation threshold is identified to be at around 8–10 wt% MWNTs, which is similar to Zhu et al.'s report [14]. However, such a high percolation threshold is quite dissimilar with those of polyepoxy [21], poly(butylene terephthalate) [28], polycarbonate [29], PVA and PmPV [30], and other systems [10, 31]. The influence of the aspect ratio of MWNTs on the percolation threshold in the PI system needs to be investigated further. In summary, the present study demonstrates that enhanced mechanical properties can be readily obtained using a simple in-situ polymerization process, which had not been consistently recognized in the literature previously [14, 15]. Uniform dispersion through an intensive mixing process and the high aspect ratios (mostly >1,000) of the MWNTs used play important roles in the high storage modulus and tensile strength.

## CONCLUSION

Polyimide-MWNT nanocomposites were successfully prepared via a simple in-situ polymerization process. The addition of acid-modified MWNTs into a polyimide matrix led to obvious improvements in the thermal, mechanical, and dielectric properties. For the nanocomposites containing 15 wt% MWNTs, the storage modulus reaches 28.457 GPa, about nine times of pristine polyimide at room temperature. The tensile strength of the PI-7 wt% MWNT nanocomposite is almost double the pristine PI. The PI polymer also gradually changes to a conductive system from an insulator at an identified percolation threshold at around 10 wt% MWNTs.

## REFERENCES

1. H. Dai, *Acc. Chem. Res.*, **35**, 1035 (2002).
2. A. Allaoui, S. Bai, H.M. Cheng, and J.B. Bai, *Compos. Sci. Technol.*, **62**, 1993 (2002).
3. H. Geng, R. Rasen, B. Zheng, H. Shimoda, L. Fleming, J. Liu, and O. Zhou, *Adv. Mater.*, **14**, 1387 (2002).
4. Z. Ounaies, C. Park, K.E. Wiseb, E.J. Siochic, and J.S. Harrisonc, *Compos. Sci. Technol.*, **63**, 1637 (2002).
5. S. Kumar, T.D. Dang, F.E. Arnold, A.R. Bhattacharyys, B.G. Min, and X. Zhang, *Macromolecules*, **35**, 9039 (2002).

 DOI 10.1002/pc

6. S. Cui, R. Canet, A. Derre, M. Couzi, and P. Delhaes, *Carbon*, **41**, 797 (2003).
7. L. Qu, Y. Lin, D.E. Hill, B. Zhou, W. Wang, X. Sun, A. Kitaygorodskiy, M. Suarez, J.W. Connell, L.F. Allard, and Y.P. Sun, *Macromolecules*, **37**, 6055 (2004).
8. M. Cadek, J.N. Coleman, V. Barron, K. Hedicke, and W.J. Blau, *Appl. Phys. Lett*., **81**, 5123 (2002).
9. M.A. López Manchado, L. Valentini, J. Biagiotti, and J.M. Kenny, *Carbon*, **43**, 1499 (2005).
10. A. Koganemaru, Y. Bin, Y. Agari, and M. Matsuo, *Adv. Funct. Mater*., **14**, 842 (2004).
11. Y. Bin, M. Kitanaka, D. Zhu, and M. Matsuo, *Macromolecules*, **36**, 6213 (2003).
12. Q. Chen, Y. Bin, and M. Matsuo, *Macromolecules*, **39**, 6528 (2006).
13. K.D. Ausman, R. Piner, O. Lourie, R.S. Ruoff, and M. Korobov, *J. Phys. Chem. B*., **104**, 8911 (2000).
14. B.K. Zhu, S.H. Xie, Z.K. Xu, and Y.Y. Xu, *Compos. Sci. Technol*, **66**, 548 (2006).
15. X. Jiang, Y. Bin, and M. Matsuo, *Polymer*, **46**, 7418 (2005).
16. M. Endo, K. Takeuchi, T. Hiraoka, T. TFuruta, T. Kasai, and X. Sun, *J. Phys. Chem. Solid*., **58**, 1707 (1997).
17. T. Ogasaware, Y. Ishida, T. Ishikawa, and R. Yokota, *Composites*, **35**, 67 (2004).
18. B.J. Ash, R.W. Siegel, and L.S. Schddler, *Marcromolecules*, **37**, 1358 (2004).
19. K. Masenelle-Varlot, E. Reynaud, G. Vigier, and J. Varlet, *J. Polym. Sci. Polym. Phys*., **40**, 272 (2002).
20. W.D. Zhang, L. Shen, I.Y. Phang, and T. Liu, *Marcromolecules*, **37**, 256 (2004).
21. S. Barrau, P. Demont, A. Peigney, C. Laurent, and C. Lacabanne, *Macromolecules*, **36**, 5187 (2003).
22. A.K. Jonscher *Nature (London)*, **267**, 673 (1977).
23. J.C. Dyre and T.B. Schroder, *Rev. Mod. Phys*., **72**, 873 (2000).
24. W.D. Kingery, H.K. Bowen, and D.R. Uhlmann, *Introduction to Ceramics*, 2nd ed., John Wiley & Sons, New York (1976).
25. D. Bergman and Y. Imry, *Mater. Phys. Rev. Lett*., **39**, 1222 (1977).
26. C.W. Nan, *Prog. Mater. Sci*., **37**, 1 (1993).
27. G.D. Liang and S.C. Tjong, *Mater. Chem. Phys*., **100**, 132 (2006).
28. A. Nogales, G. Broza, Z. Roslaniec, K. Schulte, B.S. Sics, S. Hsiao, A. Sanz, M.C. Garcia-Gutierrez, D.R. Rueda, C. Domingo, and T.A. Ezquerra, *Macromolecules*, **37**, 7669 (2004).
29. P. Pötschkea, M. Sergej, and I. Alig, *Polymer*, **44**, 5023 (2003).
30. B.E. Kilbride, J.N. Coleman, J. Fraysse, P. Fournet, M. Cadek, A. Drury, S. Hutzler, S. Roth, and W.J. Blau, *J. Appl. Phys*., **92**, 4024 (2002).
31. J.G. Smith, J.W. Connell, D.M. Delozier, P.T. Lillehei, K.A. Watson, Y. Lin, B. Zhou, and Y.P. Sun, *Polymer*, **45**, 825 (2004).